Liquid Crystals
Publication details, including instructions for authors and subscription information:
http://www.informaworld.com/smpp/title~content=t713926090

Poynting vector in a uniaxially birefringent multilayered system

R. A. Innes[a]; K. R. Welford[a]; J. R. Sambles[a]
[a] Thin Film and Interface Group, Department of Physics, University of Exeter, Stocker Road, Exeter, England

To cite this Article Innes, R. A. , Welford, K. R. and Sambles, J. R.(1987) 'Poynting vector in a uniaxially birefringent multilayered system', Liquid Crystals, 2: 6, 843 — 851
To link to this Article: DOI: 10.1080/02678298708086340
URL: http://dx.doi.org/10.1080/02678298708086340

LIQUID CRYSTALS, 1987, VOL. 2, NO. 6, 843–851

Poynting vector in a uniaxially birefringent multilayered system

by R. A. INNES, K. R. WELFORD and J. R. SAMBLES
Thin Film and Interface Group, Department of Physics, University of Exeter, Stocker Road, Exeter EX4 4QL, England

(*Received 11 June 1987; accepted 3 July 1987*)

Calculations of the Poynting vector in a uniaxially birefringent multilayered system are presented. Such calculations are then used to illustrate results from a system involving a liquid crystal layer aligned between silver films and observed using attenuated total reflection. Excitation of surface plasmon-polariton and guided wave resonances within the structure provide for highly structured reflectivity and transmissivity responses. Detailed analysis of the optical response of the layered structure are presented elsewhere. In this work the Poynting vector fields for several of the resonant modes are examined.

1. Introduction

Recently Welford and Sambles [1] presented results from a study of the reflectance of p polarized light from the multilayered system involving a nematic liquid crystal shown in figure 1. The system involves a prism ($\varepsilon \approx 3{\cdot}24$ at $\lambda = 632{\cdot}8$ nm) on to which has been evaporated a silver film (thickness ≈ 40 nm) and an aligning layer of SiO_x (thickness ≈ 20 nm) where x lies between 1 and 2. The SiO_x is evaporated in such a direction that the director of the liquid crystal lies in the plane of polarization and parallel to the interface. If an electric field is applied across the liquid crystal cell then the director will tend to align with the applied field in the plane of polarization. It is possible to show [1] that this results in a graded refractive index profile across the liquid crystal which allows waveguiding in the liquid crystal. Furthermore coupling to the surface plasmon-polariton mode along the silver–SiO_x interface may also be observed. A typical plot of reflectivity of p polarized He/Ne laser light as a function of angle of incidence in the prism is shown in figure 2, the liquid crystal in this case is subjected to an applied voltage of 7·93 V. It should be noted that both bulk guided modes and surface guided mode are observed simultaneously. The transmitted intensity as a function of incident angle was also recorded and is shown in figure 3.

A theoretical model for such a uniaxial system has been presented by Sprokel [2], in which he uses a 2×2 matrix method to calculate the reflectance as a function of angle of incidence. We have furthered this calculation to obtain the Poynting vector through this multilayered system.

2. Calculation of the Poynting vector

The theoretical model system is shown in figure 4. We use the notation of Sprokel, i.e. a positive superscript denotes a forward propagating wave and negative superscript denotes a reverse propagating wave. Since the director (optic axis) of the liquid crystal tilts in the plane of polarization (the xz plane) only the extraordinary wave

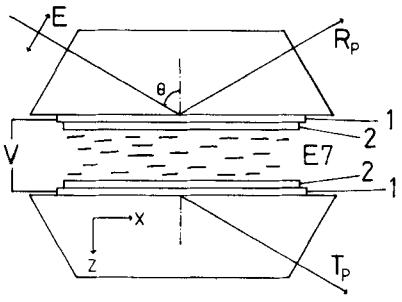

Figure 1. Typical experimental geometry showing the glass (n = 1·8) substrates coated in silver, layers 1, and silicon oxide (SiO_x), layers 2. Voltages may be applied across the nematic liquid crystal by using the silver layers as electrodes.

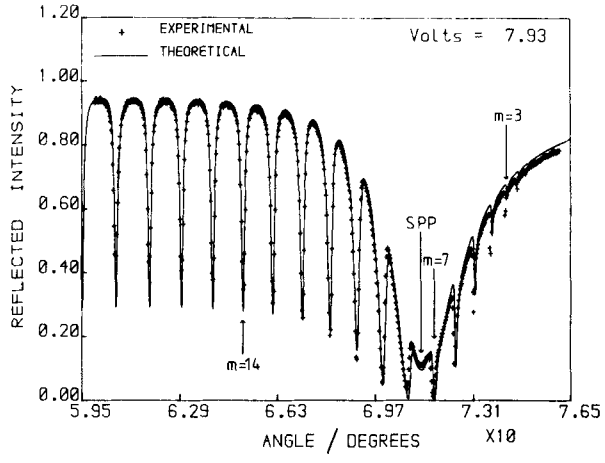

Figure 2. Attenuated total reflection signal from the nematic system at 7·93 V. The parameters used to generate the theoretical curve are given in tables 1 and 2. The angles at which the Poynting vector calculations are made are indicated with arrows.

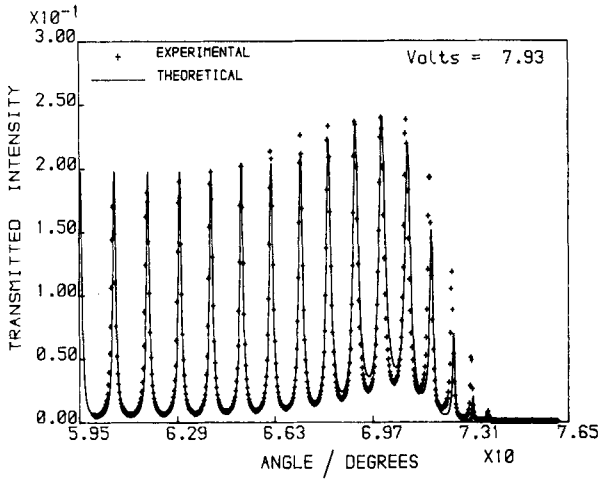

Figure 3. Transmitted signal from the nematic system. The fitting parameters are the same as those used in the reflected signal.

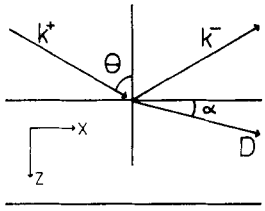

Figure 4. Schematic representation of incident and reflected waves at a uniaxial layer. The director, D, is parallel to the local optic axis and is orientated at an angle α to the interface.

Table 1. Optical parameters used in generating theoretical reflection and transmissions shown in figures 2 and 3.

Optical parameters			
	Relative permittivity		
Layer	Real	Imaginary	Thickness/nm
Prism	3·239	0·000	Infinite
Silver	−17·754	0·787	40·00
SiO_x	2·234	0·004	26·50

Table 2. Liquid crystal parameters used to generate the theoretical curves in figures 2 and 3.

Liquid crystal parameters	
Variable	Value
Ordinary index	1·518
Extraordinary index	1·741
Splay elastic constant	$11{\cdot}7 \times 10^{-12}/\mathrm{Nm}^{-1}$
Bend elastic constant	$18{\cdot}9 \times 10^{-12}/\mathrm{Nm}^{-1}$
Dielectric constant (parallel)	19·21
Dielectric constant (perpendicular)	5·08
Nematic layer thickness	9·54/μm
Surface tilt angle	9·10/degree

is excited, thus greatly simplifying the calculations. The orientation of the nematic liquid crystal director through the liquid crystal layer as a function of applied voltage is calculated using the Frank–Oseen continuum theory [3]. In its original form this theory is unable to calculate director tilt profiles at applied voltages of greater than $\sim 5V_0$, where V_0 is the critical voltage. Recently, however, Welford and Sambles [4] have developed a technique which allows nematic director tilt profiles to be calculated at any applied voltage. With this information the system is then modelled as a multilayer structure, each thin nematic liquid crystal layer having a constant tilt angle which varies from layer to layer.

Sprokel derives for us the dispersion relations for forward and reverse propagating waves in a uniaxial medium. These are

$$k_z^+ = \frac{1}{C}\{-k_x B + [\varepsilon_1 \varepsilon_2(\omega^2 C\mu_0 - k_x^2)]^{1/2}\} \quad (1)$$

and

$$k_z^- = \frac{1}{C}\{k_x B + [\varepsilon_1 \varepsilon_2(\omega^2 C\mu_0 - k_x^2)]^{1/2}\}, \tag{2}$$

where ε_1 is the dielectric constant at optical frequencies parallel to the optic axis, ε_2 is the dielectric constant perpendicular to the optic axis, and k_x and k_z are the wavevector components in the plane of incidence. In addition

$$A = \varepsilon_1 \cos^2\alpha + \varepsilon_2 \sin^2\alpha,$$

$$B = (\varepsilon_1 - \varepsilon_2)\sin\alpha\cos\alpha,$$

$$C = \varepsilon_1 \sin^2\alpha + \varepsilon_2 \cos^2\alpha,$$

where α is the angle of tilt of the director as depicted in figure 4.

Multiplication of Sprokel's final transfer matrix expression for the whole system (equation (19) of his work) by the inverse product matrix leads to the inverted form:

$$\begin{pmatrix} E_{i,x}^+ \exp(-ik_{i,z}^+ z_{i-1}) \\ E_{i,x}^- \exp(ik_{i,z}^- z_{i-1}) \end{pmatrix} = \prod_{j=1}^{j=i} N_j \begin{pmatrix} E_{0,x}^+ \\ E_{0,x}^- \end{pmatrix}, \tag{3}$$

where we have taken the first interface to be at $z = z_0 = 0$ and the last interface to be at $z = z_n$. The matrices $\mathbf{N}_j$ are given by

$$\mathbf{N}_j = \begin{pmatrix} \left(\frac{U_j + U_{j-1}}{2U_j}\right)\exp(-ik_{j-1,z}^+ d_{j-1}) & \left(\frac{U_j - U_{j-1}}{2U_j}\right)\exp(ik_{j-1,z}^- d_{j-1}) \\ \left(\frac{U_j - U_{j-1}}{2U_j}\right)\exp(-ik_{j-1,z}^+ d_{j-1}) & \left(\frac{U_j + U_{j-1}}{2U_j}\right)\exp(ik_{j-1,z}^- d_{j-1}) \end{pmatrix},$$

where

$$U_j = \omega\left(\frac{\varepsilon_1 \varepsilon_2}{\omega^2 C_j \mu_0 - k_x^2}\right)^{1/2}.$$

The product matrix $\prod_{j=1}^{j=i} \mathbf{N}_j$ may be written in the form

$$\prod_{j=1}^{j=i} \mathbf{N}_j = \begin{bmatrix} \mathbf{M}_{11,i} & \mathbf{M}_{12,i} \\ \mathbf{M}_{21,i} & \mathbf{M}_{22,i} \end{bmatrix}. \tag{4}$$

Using equations (3) and (4) we are able to express the x components of the electric fields anywhere in the systems in terms of the incident x component. That is

$$E_{i,x}^+ = \left(\mathbf{M}_{11,i} - \mathbf{M}_{12,i}\left[\frac{\mathbf{M}_{21,n}}{\mathbf{M}_{22,n}}\right]\right) E_{0,x}^+ \exp(ik_{i,z}^+ z_{i-1}) \tag{5}$$

and

$$E_{i,x}^- = \left(\mathbf{M}_{21,i} - \mathbf{M}_{22,i}\left[\frac{\mathbf{M}_{21,n}}{\mathbf{M}_{22,n}}\right]\right) E_{0,x}^+ \exp(-ik_{i,z}^+ z_{i-1}). \tag{6}$$

Elimination of H_y in equation (5) of Sprokel [2] allows E_z to be determined from E_x

$$\left.\begin{aligned} E_{i,z}^{+} &= \frac{(Ak_x + Bk_z^{+})}{(Ck_z^{+} + Bk_x)} E_{i,x}^{+} \\ \text{and} \\ E_{i,z}^{-} &= \frac{(Ak_x + Bk_z^{-})}{(Ck_z^{-} - Bk_x)} E_{i,x}^{-}. \end{aligned}\right\} \tag{7}$$

Use of equation (13) of Sprokel [2], i.e.

$$\left.\begin{aligned} H_{i,y}^{+} &= U_i E_{i,x}^{+}, \\ H_{i,y}^{-} &= -U_i E_{i,x}^{-}, \end{aligned}\right\} \tag{8}$$

gives the magnetic field components.

Equations (5), (6), (7) and (8) then allow calculation of the Poynting vector at any point through the system since

$$\left.\begin{aligned} S_x &= \mathrm{Re}(-E_z H_y^{*}) \\ \text{and} \\ S_z &= \mathrm{Re}(E_x H_y^{*}). \end{aligned}\right\} \tag{9}$$

However, before examining the Poynting vector distribution for a variety of angles of incidence we give a qualitative description of the optical properties of the system studied.

3. Qualitative description of the system

So that a full understanding of the optical behaviour of the nematic liquid crystal system can be obtained it is helpful to consider a qualitative model of the layered structure. Two quite different, but interacting, guided wave phenomena occur simultaneously. First, there is the surface guided wave, the surface plasmon-polariton, propagating along the silver–SiO_x interface, and second there is the bulk guided wave propagating in the liquid crystal material. In the first instance, without any applied voltage, the attenuated totally reflected waves excite exponentially decaying fields extending through the silver–SiO_x–liquid crystal layers. At a particular angle of incidence these fields couple strongly to the surface plasmon-polariton at the silver–SiO_x interface causing the characteristic reduction in the reflected intensity. Within the experimental structure under current investigation, in the absence of any applied field, the surface plasmon-polariton has maximum coupling at an incident angle of $\sim 69°$.

Applying a voltage across the nematic liquid crystal layer induces elastic deformations within the liquid crystal which results in a non-uniform director profile. With p polarized radiation in this layered structure the E_z field components are much stronger than the E_x field components and hence the exponentially decaying fields extending into the liquid crystal material experience an effective low–high–low refractive index profile. In short the nematic layer forms a waveguiding structure in an applied voltage. Low voltages only reorientate the central region of the nematic material and the effective refractive index difference between the guiding and cladding region is small. A low waveguiding cut-off angle and an unperturbed surface plasmon-polariton are the consequence. However, further increasing the applied voltage raises

the level of distortion of the director profile which thus increases the effective refractive index difference between the guiding and cladding region. Close to maximum cut-off angle (for E7 (BDH Chemicals Limited) about 75° in the present arrangement) is achieved at relatively low levels of director distortion, the dielectric properties of the system close to the silver–SiO_x interface being only weakly perturbed. The net result is that although the surface plasmon-polariton resonance angle has moved with the applied voltage, the guided wave resonance shift to higher angles faster so that at 7·93 V a guided wave and the surface plasmon-polariton may have the same momentum causing both resonances to occur simultaneously. Fully distorting the director profile at high voltages ($> 20V_0$) therefore tilting the director near the SiO_x interface causes the surface plasmon-polariton to be perturbed severely and moves its resonance angle beyond the waveguide cut-off angle. Modelling the nematic material as a step index waveguide using the simple transverse resonance condition and the effective indices for the guiding and cladding region predicts the correct mode spacing and the correct cut-off angle. In order to achieve the theoretical fits shown in figures 2 and 3 a full analysis is required, similar to that discussed previously by Welford and Sambles [5].

Support for this qualitative view is now provided by examining the Poynting vector at a selection of incident angles indicated in figure 2.

4. Poynting vector examination

Counting the number of minima in the Poynting vector field across the width of the waveguiding region gives the mode number. In a normal step index dielectric waveguide the lowest order mode has no minimum in the Poynting vector field and is termed the $m = 0$ mode. As we shall see this mode is too weakly coupled to in the nematic waveguide for it to be detected. If the waveguide mode has n minima it is described as the $m = n$ mode. Depicted in figure 5 is the Poynting vector field for the mode $m = 14$. In this figure, and subsequent figures of this type, distance into the layered structure is represented vertically. Each of the straight lines drawn in the xz plane represents the magnitude and direction of the Poynting vector at the z position from which it extends. The silver and SiO_x layers are represented by the very thin layers drawn parallel to the edges of the waveguiding region. Due to their small dimensions the Poynting vector fields in these layers are not presented in the figures.

Clearly, figure 5 shows a guided wave propagating along the nematic material with periodic oscillations not only in S_x but also in S_z. (Notice how the Poynting vector calculation at the largest z value has a finite S_z component and the transmitted intensity is therefore not zero, (see figure 3).) As the mode number is reduced toward $m = 7$ so the strength of both the surface plasmon-polariton resonance and the magnitude of the surface Poynting vector gradually increase. If we inspect figure 6 it is apparent that the surface Poynting vector field has not only an S_x component but also an S_z component. Hence the surface plasmon-polariton is clearly perturbed at the guided wave resonance, indicating a degree of coupling between the two resonances. Moving to a slightly greater incident angle the Poynting vector field has been calculated at the surface plasmon-polariton resonance angle (see figure 7). Here we note the expected surface Poynting vector profile comprised largely of S_x which decays exponentially into the nematic material. However, the exponential decay is not fast enough to prevent a weak coupling to a guided mode resonance. This is significant in as much as it allows transfer of power across the nematic material resulting in a weak coupling of radiation into a transmitted wave. This is not usually the case for the surface plasmon-polariton. Lowering the mode number of guided waves to $m = 3$

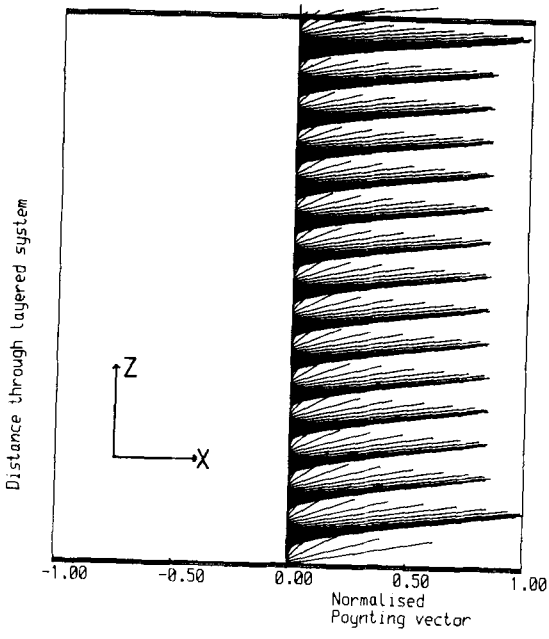

Figure 5. The Poynting vector field for the guided mode $m = 14$. Angle of incidence is 60·71° and the peak power enhancement is 5·98.

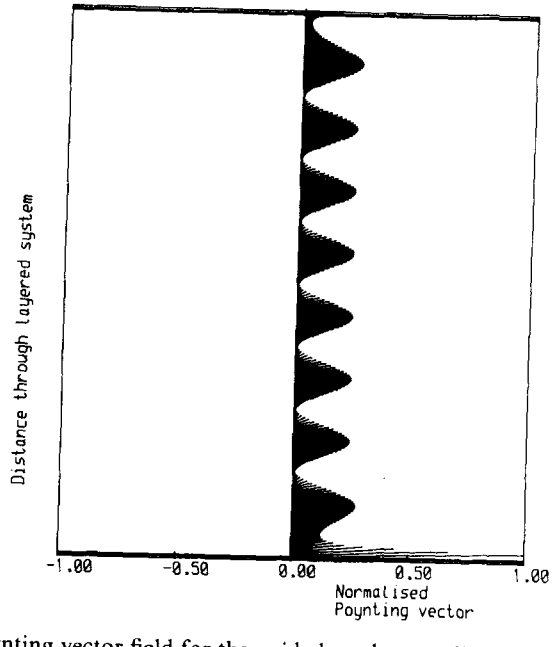

Figure 6. The Poynting vector field for the guided mode $m = 7$ excited at an incident angle of 71·79°. The surface power enhancement is 11·9 whereas the guided wave peak power enhancement is 3·13.

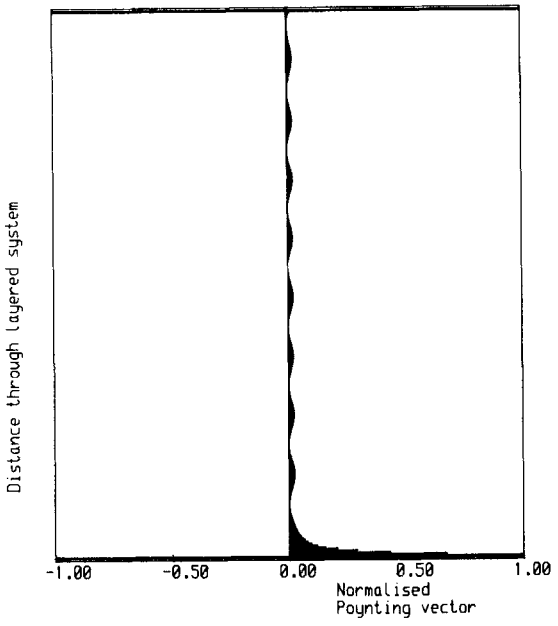

Figure 7. The Poynting vector field at the surface plasmon-polariton resonance angle, 71·32°, with a power enhancement of 18·7.

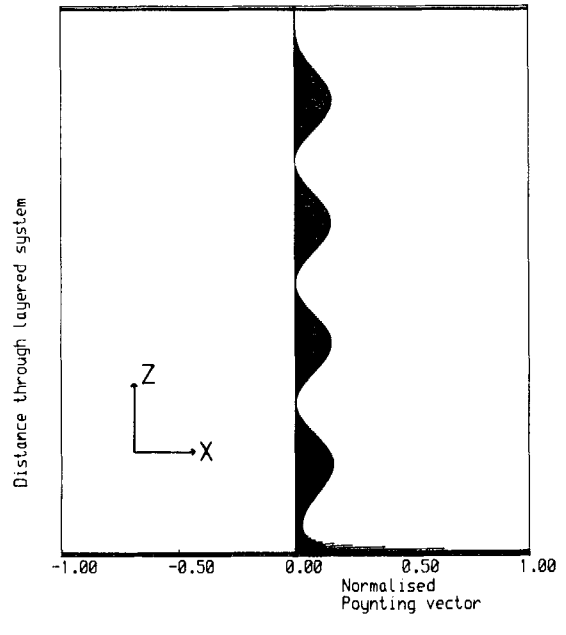

Figure 8. The Poynting vector field from the guided mode $m = 3$, calculation made at 74·31°. Power enhancements are 3·81 at the surface and 0·6 at the peaks in the waveguide.

(see figure 8) it is possible to identify surface plasmon-polariton/guided wave coupling as seen previously. However, the S_z component of the Poynting vector has vanished at the far surface of the guide, and with it the corresponding transmitted intensity.

Normalizing the Poynting vector field within the layered structure to the incident Poynting vector allows the power enhancement to be calculated. Reduction of the mode number decreases the waveguide peak power enhancement from 5·98 when $m = 18$ to $\sim 0{\cdot}6$ when $m = 3$, with a sharp surface power enhancement of 18·7 at the surface plasmon-polariton resonance angle.

5. Conclusions

We have outlined how the Poynting vector may be calculated for a uniaxially birefringent multilayered system. Such calculations have been shown to be very useful in understanding experimental results from a system involving a thin liquid crystal layer. Work is currently under way to examine the radiation distribution in more complex structures containing twisted liquid crystal in which TE and TM wave mixing occurs. This necessitates 4×4 matrix techniques and is a more elaborate procedure.

The authors gratefully acknowledge the support of the SERC both for CASE studentships (K.R.W. and R.I.), and an equipment grant. Further thanks are due to the University of Exeter for supporting K.R.W. as a research fellow.

References

[1] WELFORD, K. R., and SAMBLES, J. R., 1987, *Appl. Phys. Lett.*, **50**, 871.
[2] SPROKEL, G. J., 1981, *Molec. Crystals liq. Crystals*, **68**, 39.
[3] DUELING, H. J., 1972, *Molec. Crystals liq. Crystals*, **19**, 123.
[4] WELFORD, K. R., and SAMBLES, J. R., 1987, *Molec. Crystals liq. Crystals*, **147**, 25.
[5] WELFORD, K. R., and SAMBLES, J. R., 1987, *Liq. Crystals*, **2**, 91.